Received: 12 January 2022 | Revised: 15 March 2022 | Accepted: 19 March 2022

DOI: 10.1111/cas.15346

ORIGINAL ARTICLE

Cancer Science WILEY

Insufficiency of hepatocyte growth factor activator inhibitor-1 confers lymphatic invasion of tongue carcinoma cells

Aya Izumi[1] | Koji Yamamoto[1] | Makiko Kawaguchi[1] | Fumiki Yamashita[1] | Tsuyoshi Fukushima[1] | Takumi Kiwaki[1] | Hiroyuki Tanaka[1] | Yoshihiro Yamashita[2] | Hiroaki Kataoka[1]

[1]Section of Oncopathology and Regenerative Biology, Department of Pathology, Faculty of Medicine, University of Miyazaki, Miyazaki, Japan

[2]Department of Oral and Maxillofacial Surgery, Faculty of Medicine, University of Miyazaki, Miyazaki, Japan

Correspondence
Hiroaki Kataoka, Section of Oncopathology and Regenerative Biology, Department of Pathology, Faculty of Medicine, University of Miyazaki, 5200 Kihara, Kiyotake, Miyazaki 889-1692, Japan.
Email: mejina@med.miyazaki-u.ac.jp

Funding information
Japan Society for the Promotion of Science, Grant/Award Number: 16H05175 and 20K18483

Abstract

Hepatocyte growth factor (HGF) activator inhibitor type-1 (HAI-1), encoded by the *SPINT1* gene, is a transmembrane protease inhibitor that regulates membrane-anchored serine proteases, particularly matriptase. Here, we explored the role of HAI-1 in tongue squamous cell carcinoma (TSCC) cells. An immunohistochemical study of HAI-1 in surgically resected TSCC revealed the cell surface immunoreactivity of HAI-1 in the main portion of the tumor. The immunoreactivity decreased in the infiltrative front, and this decrease correlated with enhanced lymphatic invasion as judged by podoplanin immunostaining. In vitro homozygous deletion of *SPINT1* (HAI-1KO) in TSCC cell lines (HSC3 and SAS) suppressed the cell growth rate but significantly enhanced invasion in vitro. The loss of HAI-1 resulted in enhanced pericellular activities of proteases, such as matriptase and urokinase-type plasminogen activator, which induced activation of HGF/MET signaling in the co-culture with pro-HGF-expressing fibroblasts and plasminogen-dependent plasmin generation, respectively. The enhanced plasminogen-dependent plasmin generation was abrogated partly by matriptase silencing. Culture supernatants of HAI-1KO cells had enhanced potency for converting the proform of vascular endothelial growth factor-C (VEGF-C), a lymphangiogenesis factor, into the mature form in a plasminogen-dependent manner. Furthermore, HGF significantly stimulated VEGF-C expression in TSCC cells. Orthotopic xenotransplantation into nude mouse tongue revealed enhanced lymphatic invasion of HAI-1KO TSCC cells compared to control cells. Our results suggest that HAI-1 insufficiency leads to dysregulated pericellular protease activity, which eventually orchestrates robust activation of protease-dependent growth factors, such as HGF and VEGF-C, in a tumor microenvironment to contribute to TSCC progression.

KEYWORDS
HAI-1, HGF, matriptase, oral squamous cell carcinoma, VEGF-C

Aya Izumi and Koji Yamamoto contributed equally.

1 | INTRODUCTION

Squamous cell carcinoma is the major histological type of oral cancer. It is highly frequent in South Central Asia and ranks 18th in incidence of cancers worldwide.[1] Tongue squamous cell carcinoma (TSCC) accounts for approximately 40% of oral cancers.[2] Although early stage TSCC is usually amenable to surgery, most patients present at an advanced disease stage. Surgical techniques, chemoradiotherapy and several other targeted therapies have advanced over the past two decades, but the 5-year survival rate for TSCC patients is still below 50%.[3] Rapid local invasion and lymph node metastasis are the main challenges in managing TSCC, and the underlying mechanisms of the aggressive features of this disease remain unclear.

Hepatocyte growth factor (HGF) activator inhibitor type-1 (HAI-1) is a type I transmembrane Kunitz-type serine protease inhibitor. HAI-1 is expressed in most epithelial cells and placenta trophoblasts.[4] Initially identified as an endogenous inhibitor of serum HGF activator,[5] type II transmembrane serine proteases (TTSPs) and glycosylphosphatidylinositol-anchored serine protease prostasin are physiological targets of HAI-1 in epithelial cells.[4,6] Among TTSPs, matriptase has been identified as the cognate target protease of HAI-1.[4,6,7] Abnormal matriptase activity contributes to the development and progression of squamous cell carcinoma of the skin.[8–10]

Matriptase and HGF activator stimulate extracellular activation of the proform of HGF (pro-HGF).[4,11] Mature HGF activates the MET tyrosine kinase receptor pathway, which contributes to multiple cellular processes in cancers, including invasion, metastasis, and angiogenesis as well as protection from apoptosis.[12–14] Other growth factors, such as platelet-derived growth factor-C and -D and macrophage stimulating protein (a ligand of RON tyrosine kinase receptor), are activated by matriptase,[15–17] as are protease-activated receptor-2 (PAR-2) and other protease zymogens, such as the proform of urokinase-type plasminogen activator (pro-uPA).[18–21] Together, these targets of HAI-1 contribute to neoplastic progression, and consequently, accumulating experimental evidence has indicated suppressive roles for HAI-1 in carcinogenesis and metastasis.[4,8,22–25]

We have reported that HAI-1 immunoreactivity in oral cancer tended to be reduced at the invasion front of infiltrating-type cancers and was accompanied by increased numbers of cancer-associated fibroblasts through enhanced activation of matriptase/PAR-2 axis[21] and increased risk of lymph node metastasis.[26] However, the molecular mechanism underpinning the increased risk of lymph node metastasis associated with decreased HAI-1 remains to be clarified. In this study, we examined the effects of HAI-1 loss on the invasive growth of TSCC cells in vitro as well as on tumorigenesis, lymphatic invasion and lymph node metastasis in vivo using an orthotopic xenotransplantation method. Our results suggested that HAI-1 deficiency induced dysregulated pericellular protease activities that eventually promoted robust activation of growth factors possibly involved in lymphangiogenesis and invasion in the context of the tumor microenvironment.

2 | MATERIALS & METHODS

2.1 | Antibodies

The following antibodies were used: anti-human HAI-1 rabbit mAb (ab189511; Abcam), anti-human podoplanin mouse mAb (clone D2-40, M3619; DAKO), anti-mouse podoplanin hamster mAb (DM3501; OriGene), anti-human vascular endothelial growth factor-C (VEGF-C) goat polyclonal Ab (AF752; R&D systems), anti-phosphorylated (Tyr1234/1235) MET rabbit mAb (#3077; Cell Signaling), and anti-human β-actin mouse mAb (Sigma). Anti-human MET mouse mAb and anti-human matriptase mAb (M24) were kindly provided by the Yokohama Research Center, Mitsubishi Pharma and Dr Chen-Yong Lin (Lombardi Cancer Center, Georgetown University), respectively.[7,27]

2.2 | Clinicopathological study cohort

The study protocol was in accordance with the revised Helsinki Declaration of 1983 and approved by the Institutional Review Board of the Faculty of Medicine, University of Miyazaki (approval number: 2014–006). A total of 42 Japanese patients were included in this study, and they did not receive adjuvant therapy prior to surgery. All patients underwent surgery at the University of Miyazaki Hospital between April 2000 and November 2014. The patients were between 28 and 96 years old. The mean and median patient age was 64.1 and 67 years old, respectively. Paraffin-embedded tissue sections of the resected tumor tissues were processed for H&E staining and immunohistochemical staining.

2.3 | Immunohistochemical study

Immunohistochemistry of paraffin embedded tissues was performed as described previously.[26,28] The HAI-1 immunoreactivity score was calculated as the sum of the following point values: cytoplasmic staining in >50% of tumor cells, 0.5 point; distinct membranous staining in 20%–50% of tumor cells, 1 point; and distinct membranous staining in >50% of tumor cells, 2 points. The immunoreactivity score of the whole tumor tissue was compared with that of the tumor invasion front. Then, the degree of reduction of HAI-1 levels in the invasion front (HAI-1 reduction level) was calculated by subtracting the invasion front HAI-1 score from the whole tumor area HAI-1 score.[26] Lymphatic permeation of cancer cells and the number of lymph vessels were evaluated by podoplanin immunohistochemistry.

2.4 | Cell culture

Human TSCC cell lines, HSC3 and SAS, were obtained from the Riken Cell Bank and the Cell Resources Center for Research

(Tohoku University, Sendai, Japan), respectively. The human embryonic kidney cell line, HEK293T, and human fibroblast cell line, MRC5, were from the Riken Cell Bank and the Japanese Cancer Research Resources Bank, respectively, and cultured in DMEM containing 10% FBS (Sigma) at 7°C in a fully humidified atmosphere of 5% CO_2 in air.

2.5 | Knockout of the *SPINT1* gene and knockdown of matriptase in cultured cells

Genome editing using clustered regularly interspaced short palindromic repeat (CRISPR)/CRISPR-associated proteins 9 (Cas9) was applied for *SPINT1* (HAI-1) gene knockout (KO) in the HSC3 cell line and the SAS cell line as described previously.[29] KO of the *SPINT1* gene was confirmed by genome sequencing and immunoblot analysis. For transient silencing of matriptase, two kinds of siRNA (siMat#1 and siMat#2; Table S1) were used as described.[21] Transfection of siRNA was performed using the RNAiMax reagent (Invitrogen).

2.6 | Evaluation of cellular proliferation, migration, and invasion

Cell proliferation was evaluated using CCK-8 (DOJINDO Laboratories) according to the manufacturer's instructions. For the colony forming assay, cells were seeded into six-well plates at 100 cells per well and cultured for 10 days. Plates containing colonies were washed with PBS and fixed, followed by staining with crystal violet. The number of visible colonies was counted, and the size of each colony was measured by microscopy. A wound healing assay was used to determine cellular migration activity, as described prevously.[29] To evaluate the invasive activity, trans-well chambers (ThinCert, Greiner Bio-One) were coated with 25 μg/filter of Matrigel (BD Biosciences). A total of 1×10^5 cells suspended in DMEM with 0.1% BSA were seeded in the upper chamber. The lower chamber was filled with medium supplemented with 5% FBS. Cells were incubated at 37° for 24 h and invading cells on the inferior surface of the filters were fixed and stained with hematoxylin.

2.7 | Protease activity assays

To measure matriptase activity, serum-free culture conditioned medium was mixed with the synthetic substrate Boc-Glu-Ala-Arg-AMC (Peptide Institute; 10 μM). Fluorescence release was measured using a FlexStation 3 (Molecular Devices) for 30 min at 37°C, and the velocity max was calculated. Pericellular activities of urokinase-type plasminogen activator (uPA) and plasmin were measured with the synthetic substrates S-2444 (pyro-Glu-Gly-Arg-p-nitroanilide) and S-2251 (H-D-Val-Leu-Lys-p-nitroanilide dihydrochloride), respectively (KabiVitrum). Briefly, after the cells reached 80% confluency in the 96-well plate, each well was washed with PBS three times. For uPA activity assay, each well was filled with 100 μL PBS containing 10 μg/mL S-2444 and incubated for 90 min at 37°C. For plasmin activity assay, cells in 96-well plates were pretreated with 1 μg/mL plasminogen (R&D systems) for 3 h and then incubated with 10 μg/mL S-2251 for 90 min at 37°C. After incubation, optical density at 405 nm of each well was measured.

2.8 | Immunoblotting, RT-PCR and quantitative RT-PCR

Cell lysates were collected in 1% Triton X-100 in PBS with protease inhibitor cocktail (Sigma). Equal amounts of proteins were subjected to standard SDS-PAGE and processed for a standard immunoblot analysis as described previously.[29] The labeled proteins were visualized with a chemiluminescence reagent (PerkinElmer Life Sciences). RT-PCR and quantitative real-time RT-PCR were performed as described previously.[21] The primer sequences were indicated in Table S1.

2.9 | Vascular endothelial growth factor-C processing assay and hepatocyte growth factor

For preparation of recombinant pro-VEGF-C, HEK293T cells were transfected with plasmids encoding full-length FLAG-tagged VEGF-C (OriGene) using Lipofectamine 3000 (Invitrogen), cultured in HE100 medium (Gmep), and the conditioned medium was collected 48 h after transfection. Then, the medium was concentrated via ultrafiltration before overnight dialysis at 4°C in PBS. FLAG-tagged VEGF-C was immunopurified by column chromatography using DDDDK-tag protein purification cartilage (MBL). Protein purity was evaluated by SDS-PAGE followed by silver staining. For the plasminogen-dependent activation of pro-VEGF-C, serum-free culture supernatant was incubated with 2 nM plasminogen (R&D systems) for 2 h, followed by incubation with 200 nM pro-VEGF-C for 1 h at 37°C. For a positive control of processing, 200 nM pro-VEGF-C was treated with 2 nM plasmin in TBS with 5 mM $CaCl_2$ for 1 h at 37°C. To test the effect of matriptase on pro-VEGF-C processing, 200 nM pro-VEGF-C was treated with 2 nM recombinant matriptase (R&D systems) in TBS with 0.01% CHAPS. The processing was verified by immunoblotting under reducing condition. Recombinant HGF was kindly provided by Dr Takeshi Shimomura (Mitsubishi Tanabe Pharma).

2.10 | Animal experiments

All the animal work was performed using protocols approved by the University of Miyazaki Animal Research Committee, in accordance

with international guidelines for biochemical research involving animals. For the present study, 3×10^5 of HSC3 or SAS cells were laterally implanted into the muscle layer of tongues of 6 week-old male nude mice (BALB/cAJc1-nu; Kyudo) with or without 3×10^5 MRC5 fibroblasts. During the observation period, the body weight was measured every 2 days until the animals were killed based on weight loss (>20% of preinjected weight) or study timeline criteria. After study termination at 21 days, all mice were killed using somnopentyl, and the tongues, cervical lymph nodes, lungs, and livers were collected. The tissues were fixed with 10% formalin in PBS, and paraffin-embedded sections were prepared. The tumor size was evaluated as the ratio of the tumor area to the whole tongue area in an H&E section prepared from a cut surface that showed the maximum tumor diameter.

2.11 | Statistical analysis

Comparisons between two groups were performed with the Mann–Whitney *U*-test, Student's *t*-test or ANOVA with Fisher's protected least significant difference (PLSD) test. Survival curves were plotted according to the Kaplan–Meier method, and a log-rank test was used to compare survival rates. For box plot figures, the 25th and 75th percentile (boxes) and the median (bold line within the boxes) were indicated. Statistical analysis was done using the StatView 5.0 program (SAS). Significance was set at $P < 0.05$.

3 | RESULTS

3.1 | Cell surface HAI-1 immunoreactivity is decreased in cancer cells at the invasion front of tongue squamous cell carcinoma

Initially, we performed an immunohistochemical study of HAI-1 using formalin-fixed paraffin-embedded tissue sections from 42 surgically resected TSCC cases. The cancer cells in the main tumor portion generally showed obvious cell surface HAI-1 immunoreactivity, particularly in well-differentiated carcinomas. In contrast, infiltrating cancer cells at the invasion front frequently showed decreased membranous HAI-1 immunoreactivity (Figure 1A,B). We semi-quantitatively assessed the decrease in HAI-1 immunoreactivity at the invasion front (i.e., HAI-1 reduction level) and performed correlation analysis with each clinicopathological parameter. The HAI-1 reduction level was correlated with the presence of lymphatic invasion, as judged by immunohistochemistry of podoplanin ($P = 0.008$; Figure 1C and Table 1). Although tumors with a high degree of reduction in HAI-1 levels at the invasion front tended to show less differentiated morphology as well as lymph node metastasis at the time of surgery, the correlations were not statistically significant ($P = 0.0721$ and 0.0927, respectively; Table 1).

3.2 | Loss of HAI-1 suppressed growth but enhanced invasion of tongue squamous cell carcinoma cells in vitro

To clarify the role of HAI-1 in TSCC, we generated *SPINT1*$^{-/-}$ (HAI-1KO) sublines from HSC3 and SAS cell lines. Two HAI-1KO sublines and a control mock-transfected subline were obtained from HSC3 (HSC3/HAI-1KO#1, HSC3/HAI-1KO#2; Figure 2A and Figure S1). The establishment of a *SPINT1*-deleted SAS subline (SAS/HAI-1KO) and a mock-transfected control subline (Figure 2A) has been reported previously.[29] We then analyzed the role of HAI-1 in TSCC cell proliferation in vitro. The growth rate of both HSC3 and SAS cells was significantly reduced by the complete loss of HAI-1 (Figure 2B). In a colony forming assay, the colony number was not altered by loss of HAI-1, but the colony sizes of HAI-1KO cells were significantly smaller than those of control cells (Figure 2C).

We next analyzed the effects of HAI-1 loss on the migration and invasion of TSCC cells. Wound healing assays showed that HAI-1 loss significantly enhanced migration of both HSC3 and SAS cells (Figure 3A). Similarly, in vitro Matrigel invasion was significantly enhanced by the loss of HAI-1 (Figure 3B).

3.3 | Enhanced pericellular proteinase activities in the absence of HAI-1

Hepatocyte growth factor activator inhibitor type-1 insufficiency is reported to result in enhanced activity of matriptase in keratinocytes and cancer cells, including SAS.[26,30] In fact, both HSC3 and SAS cell lines and their sublines expressed matriptase (Figure 4A), and hydrolysis of the synthetic matriptase substrate Boc-Glu-Ala-Arg-AMC was increased in the absence of HAI-1 (Figure 4A). As matriptase is known to activate other zymogens, such as pro-uPA,[18–20] and considering the well-established pro-invasive roles of uPA in many cancers,[31] we then analyzed the effects of HAI-1 loss on pericellular uPA activity using the synthetic substrate S-2444. Both HSC3 and SAS cell lines expressed uPA and uPA receptor mRNAs (Figure 4A), and pericellular S-2444 hydrolysis was significantly enhanced by the loss of HAI-1 (Figure 4B). Consequently, higher plasmin activity was induced by the addition of exogenous plasminogen in HAI-1KO TSCC sublines compared to control sublines (Figure S2 and Figure 4C). This induction was inhibited, at least in part, by siRNA-mediated silencing of matriptase (Figure 4C).

3.4 | HAI-1 insufficiency confers activation of growth factors related to lymphangiogenesis

Considering the observed correlation between HAI-1 reduction level and the presence of lymphatic invasion in TSCC tissues, we then explored the possible effects of enhanced protease activities in the absence of HAI-1 on growth factors that are known to be involved in invasion and lymphangiogenesis. As the expression of

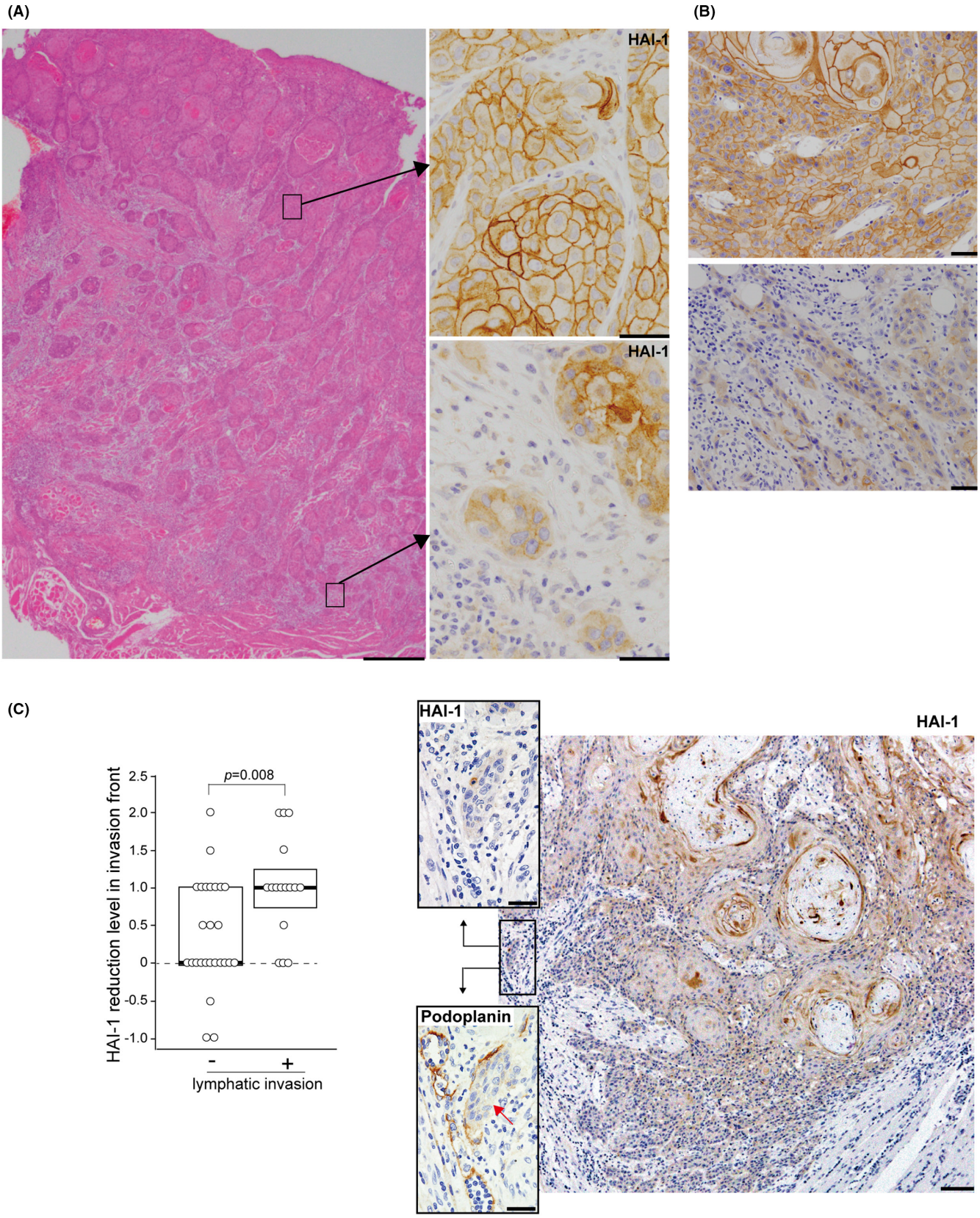

FIGURE 1 Hepatocyte growth factor activator inhibitor type-1 (HAI-1) immunoreactivity in tongue squamous cell carcinoma (TSCC) tissues. (A) A low magnification H&E-stained photo of a representative case. Insets indicate the HAI-1 immunoreactivity at the main tumor portion and invasion front. Bars, 500 μm (H&E) and 50 μm (HAI-1). (B) HAI-1 immunohistochemistry of another TSCC case, showing strong membranous immunoreactivity in the central portion (upper panel) and decreased immunoreactivity at the invasion front (lower panel). Bars, 50 μm. (C) Relationship of HAI-1 reduction level to the presence or absence of lymphatic invasion judged by anti-podoplanin (clone D2-40) immunostaining. *P*-value; Mann–Whitney *U*-test. Representative images of HAI-1 and podoplanin immunohistochemistry are also shown. Cancer cells invading a lymph vessel (red arrow) show decreased HAI-1. Bars, 150 μm and 50 μm for the main panel and insets, respectively

TABLE 1 Correlation between hepatocyte growth factor activator inhibitor type-1 (HAI-1) reduction level and clinicopathological parameters

Parameters		Number of patients	HAI−1 reduction level median (interquartile range)	*P*-values
Gender	Male	27	0.5 (0–1.0)	0.1423
	Female	15	1.0 (0.5–1.0)	
Age	>Mean (64.1)	23	1.0 (0–1.0)	0.5792
	<Mean	19	0.5 (0–1.0)	
T stage	T3 + T4	5	0 (0–1.0)	0.7919
	T1 + T2	37	1 (0–1.0)	
Lymph node metastasis at surgery	Yes	9	1.0 (0.5–1.5)	0.0927
	No	33	0.5 (0–1.0)	
Lymphatic invasion	Yes	16	1.0 (0.875–1.125)	**0.0080**
	No	26	0 (0–1.0)	
Clinical disease stage	III + IV	12	1.0 (0–1.625)	0.2387
	I + II	30	0.5 (0–1.0)	
Adjuvant therapy	Yes	23	0.5 (0–1.0)	0.4086
	No	19	1.0 (0–1.0)	
Tumor histological grade	Mod. + Poor	14	1.0 (0.125–1.375)	0.0721
	Well	28	0.5 (0–1.0)	

Note: Statistically significant *P*-values is indicated in bold.

MET, the specific receptor for HGF, is reportedly associated with VEGF-C expression and lymphangiogenesis in oral cancers and most target proteases of HAI-1 activate pro-HGF,[4,32] we explored the effect of HAI-1 loss on HGF-dependent MET phosphorylation. RT-PCR analysis indicated that both HSC3 and SAS cell lines did not express HGF mRNA (Figure 5A). Thus, we co-cultured these cell lines with the MRC5 fibroblast cell line that produces pro-HGF. HSC3 cells showed MRC5-dependent MET phosphorylation, which was significantly enhanced in HAI-1KO sublines (Figure 5B), suggesting that enhanced activation of pro-HGF produced by MRC5 occurred with the loss of HAI-1 and thereby activated HGF/MET signaling. In contrast, SAS cells showed steady-state MET phosphorylation in the absence of MRC5, which was not apparently augmented by HAI-1 loss (Figure 5C).

Next, we analyzed the expression of two major lymphangiogenesis factors, VEGF-C and VEGF-D in TSCC cells. Both HSC3 and SAS cell lines preferentially expressed VEGF-C (Figure 6A). Recombinant mature HGF significantly stimulated VEGF-C expression of the TSCC cell lines and their sublines (Figure 6B). Of note, although SAS cells showed consistent MET phosphorylation even in the absence of exogenous HGF (Figure 5C), addition of HGF enhanced the VEGF-C expression. This observation may be consistent with a previous report that the canonical HGF/MET signaling augmented intracellular MET signaling even in cells with activated MET mutation.[33] VEGF-C is secreted as a non-active proform (pro-VEGF-C), and proteolytic activation of pro-VEGF-C is required to transduce its activity through VEGF receptor-3 (VEGFR-3).[34] Plasmin is a well-known activator of pro-VEGF-C, which generates N-terminal active fragment around 20 kDa.[34,35] The culture supernatants of HAI-1KO sublines cleaved pro-VEGF-C in the presence of plasminogen, generating a presumed active VEGF-C fragment that was similar to that seen for plasmin treatment (Figure 6C).[34] This activity was barely detectable in the supernatant of control sublines or in the absence of plasminogen (Figure 6C). In addition, recombinant matriptase did not generate the N-terminal activated fragment (Figure S3). These observations suggested that HAI-1 loss induced pericellular protease activities that activated HGF and VEGF-C pathways in the tumor microenvironment in vivo, where stromal pro-HGF and serum-derived plasminogen are expected to be present. Moreover, HGF/MET signaling may amplify VEGF-C-mediated lymphangiogenesis via upregulation of VEGF-C expression.

3.5 | Orthotopic xenotransplantation of tongue squamous cell carcinoma cells indicated enhanced tumor growth and lymphatic invasion in the absence of HAI-1

Finally, we examined the effect of HAI-1 deficiency on TSCC cells in vivo. Because subcutaneous transplantation of HSC3 in nude mice was unsuccessful in our previous work,[26] here we applied an orthotopic intra-tongue transplantation method. Considering the potential harm and benefit associated with intra-tongue xenotransplantation experiments on mice, mice were killed based on weight loss (>20% of preinjected weight) or study timeline criteria (i.e., 21 days after transplantation; Table 2). The tumor size at the time of sacrifice was significantly larger in both HAI-1KO SAS and HSC3 sublines compared to corresponding control sublines

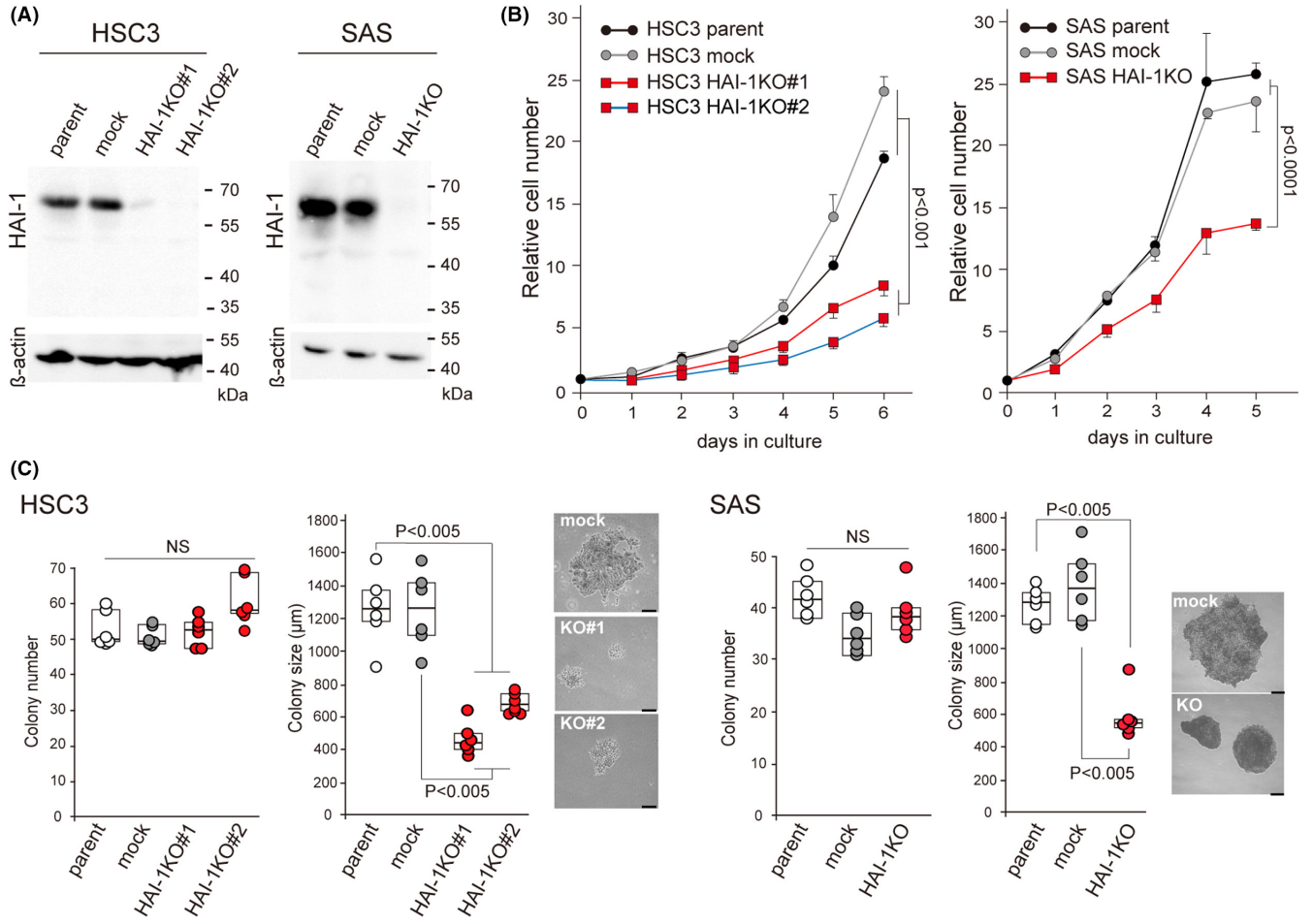

FIGURE 2 Effects of hepatocyte growth factor activator inhibitor type-1 (HAI-1) deficiency on the proliferation of HSC3 and SAS cell lines and their sublines in vitro. (A) Immunoblot analysis of HAI-1 expression in *SPINT1*$^{-/-}$ (HAI-1KO) sublines generated by genome editing. Validation of the genomic sequences is shown in Figure S1. (B) Effects of HAI-1KO on cellular growth. Values are mean ± SD ($n = 3$). *p*-values, ANOVA with Fisher's protected least significant difference (PLSD) test. (C) Effect of HAI-1KO on colony-forming efficiency. Box plot data of maximum diameter of colony (right graph) are shown. *p*-values, Mann–Whitney *U*-test ($n = 6$, for each group). NS, not significant. Representative images of the colonies are also shown. Bar, 300 μm

(Figure 7A). Unlike SAS, HSC3 cells showed stromal pro-HGF-dependent MET phosphorylation, as evidenced by the co-culture study with MRC5 human fibroblasts (Figure 5B). As murine HGF does not efficiently transduce signals through human MET,[36] we also performed a co-xenotransplantation experiment with HSC3 and MRC5 cells. As expected, co-transplantation of MRC5 promoted MET phosphorylation of HSC3 cells (Figure 7B). The number of lymphatic invasion foci was significantly increased in HAI-1KO groups compared to the control group, particularly in the model of HSC3+MRC5 co-culture (Figure 7C). The number of lymph vessels tended to be increased by the loss of HAI-1, which was statistically significant in SAS cells (Figure S4). With SAS cell transplantation, the incidence of lymph node metastasis at the time of termination (21 days after transplantation) was higher for the HAI-1KO group (9/10) compared to the control group (5/10), although this difference did not reach statistical significance ($P = 0.0571$). Although loss of HAI-1 may enhance lymph node metastasis of HSC3 cells (Table 2), 33% and 50%–70% in the mice in HSC3/HAI-1KO group and the HSC3/HAI-1KO+MRC5 co-transplantation group, respectively, were euthanized due to weight loss. Thus, we could not evaluate and compare the precise incidence of lymph node metastasis of the HSC3 sublines. In addition, we observed HAI-1 reduction at the invasion front of control HSC3 cells co-transplanted with MRC5, which likely mimicked the in vivo tumor microenvironment of human TSCC. The HAI-1 reduction level tended to correlate with the frequency of lymphatic invasion (Figure 7D). Kaplan–Meier survival analysis indicated that the loss of HAI-1 resulted in worse survival when HSC3 cells were co-transplanted with MRC5 cells (Figure 8).

4 | DISCUSSION

Hepatocyte growth factor activator inhibitor type-1/*SPINT1* is a membrane-anchored Kunitz-type serine protease inhibitor expressed on the surface of normal and neoplastic epithelial cells.

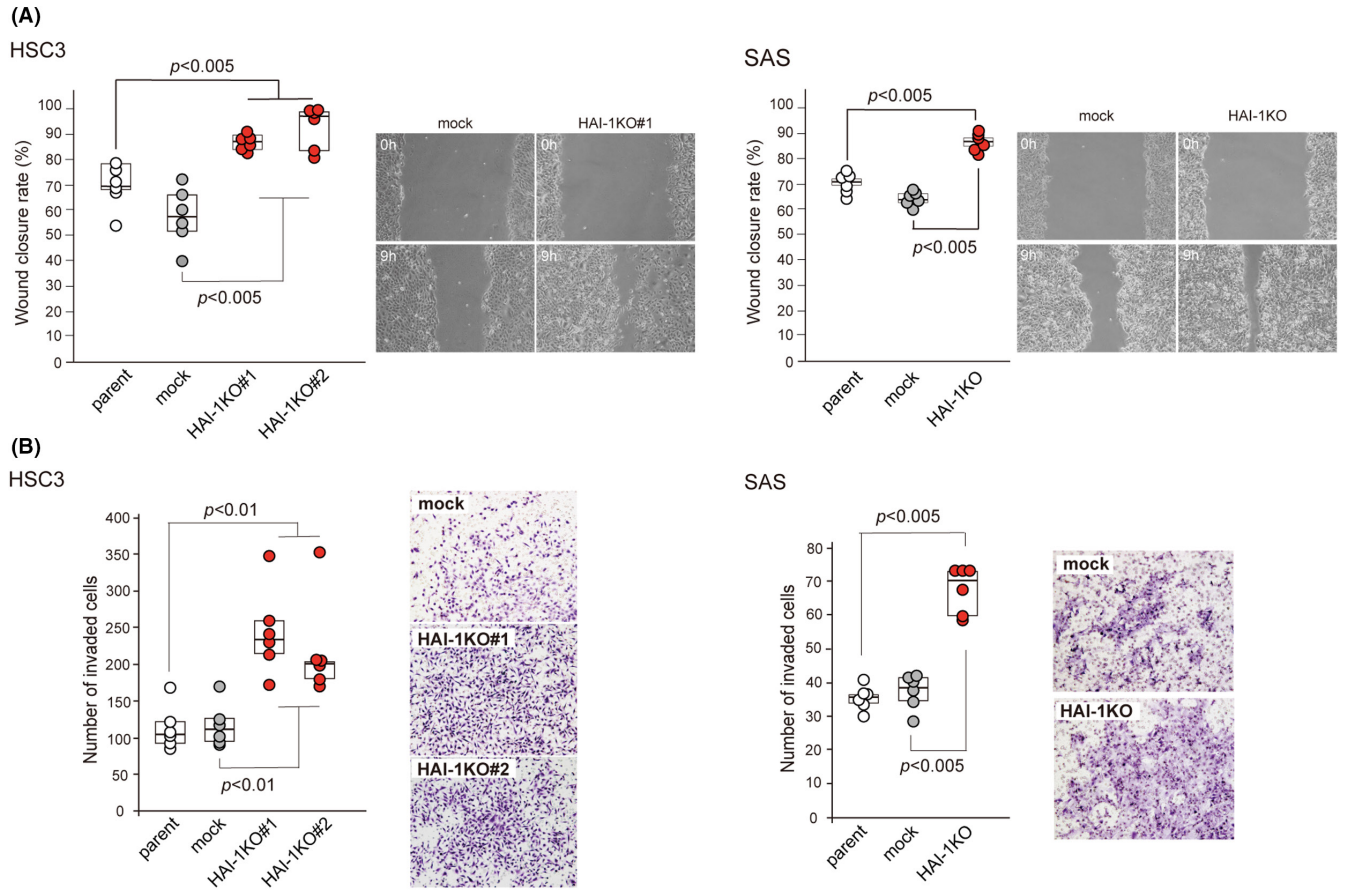

FIGURE 3 Effects of hepatocyte growth factor activator inhibitor type-1 (HAI-1) deficiency on the migration (A) and invasion (B) of HSC3 and SAS cell lines and their sublines in vitro. (A) Wound healing assay. Cells was scratched with a sterile pipette tip, washed, and cultured in serum-free DMEM. At 9 h after scratching, the wounds were measured ($n = 6$, for each group). Representative images of the assay are also shown. (B) Matrigel invasion assay ($n = 6$). *p*-values (A,B), Mann–Whitney *U*-test

In cancer cells, HAI-1 regulates the activities of cellular TTSPs, such as matriptase, hepsin and TMPRSS4, as well as serum HGF activator, most of which are known to activate pro-HGF in the pericellular microenvironment.[4] Among these TTSPs, matriptase is the most-studied cognate protease of HAI-1 in trophoblasts, keratinocytes and cancer cells.[4,6] Indeed, impaired placental development[37] and lethal skin phenotypes[38] caused by the deletion of the *Spint1* gene (i.e., Hai-1KO) in mice can be rescued by concomitant deletion or silencing of the *St14* gene encoding matriptase.[30,39,40] Furthermore, matriptase is an oncogenic protein in keratinocytes. Transgenic expression of matriptase in keratinocytes promoted neoplastic progression to develop squamous cell carcinoma, and this progression could be inhibited by the co-expression of HAI-1.[8]

In this study, we analyzed the roles of HAI-1 in invasive growth and lymphatic invasion of TSCC, a major subtype of oral cancers. Immunohistochemical analysis confirmed that TSCC cells at the invasion front tended to show decreased levels of cell surface HAI-1. The reduction of cell surface HAI-1 can be caused either by decreased transcription, post-transcriptional modulation, or enhanced shedding from the surface. We hypothesize that the enhanced shedding is the most likely mechanism underpinning the reduction in TSCC. In fact, the ectodomain shedding was responsible for the decreased membranous Hai-1 along with progression of intestinal tumors of $Apc^{Min/+}$ mice.[22] In cancer cells, membrane type-1 matrix metalloprotease (MMP14) and MMP7 reportedly cleave and release cell surface HAI-1.[22,41,42] Considering the well-established roles of MMP14 and MMP7 in cancer cell invasion,[43] it is reasonable to postulate that MMP-mediated shedding of HAI-1 occurs in the invasive TSCC cells. The current results indicated that the reduced HAI-1 levels were correlated with the presence of lymphatic invasion. To further explore the impact of HAI-1 insufficiency on TSCC cells and the lymphatic invasion activity of these cells, we generated HAI-1-deficient TSCC sublines (HSC3/HAI-1KO and SAS/HAI-1KO) by CRISPR/Cas9-based genome editing. The HAI-1KO sublines showed significantly increased cellular migration and invasion, although the growth rate was suppressed. These observations are consistent with previous reports indicating that the knockdown of HAI-1 induced epithelial to mesenchymal transition of carcinoma cells.[23,26] In this study, loss of HAI-1 resulted in enhanced pericellular protease activities, including matriptase and uPA, which contributed to subsequent activation of HGF/MET signaling and VEGF-C in the presence of pro-HGF and plasminogen, respectively. As HAI-1 cannot inhibit

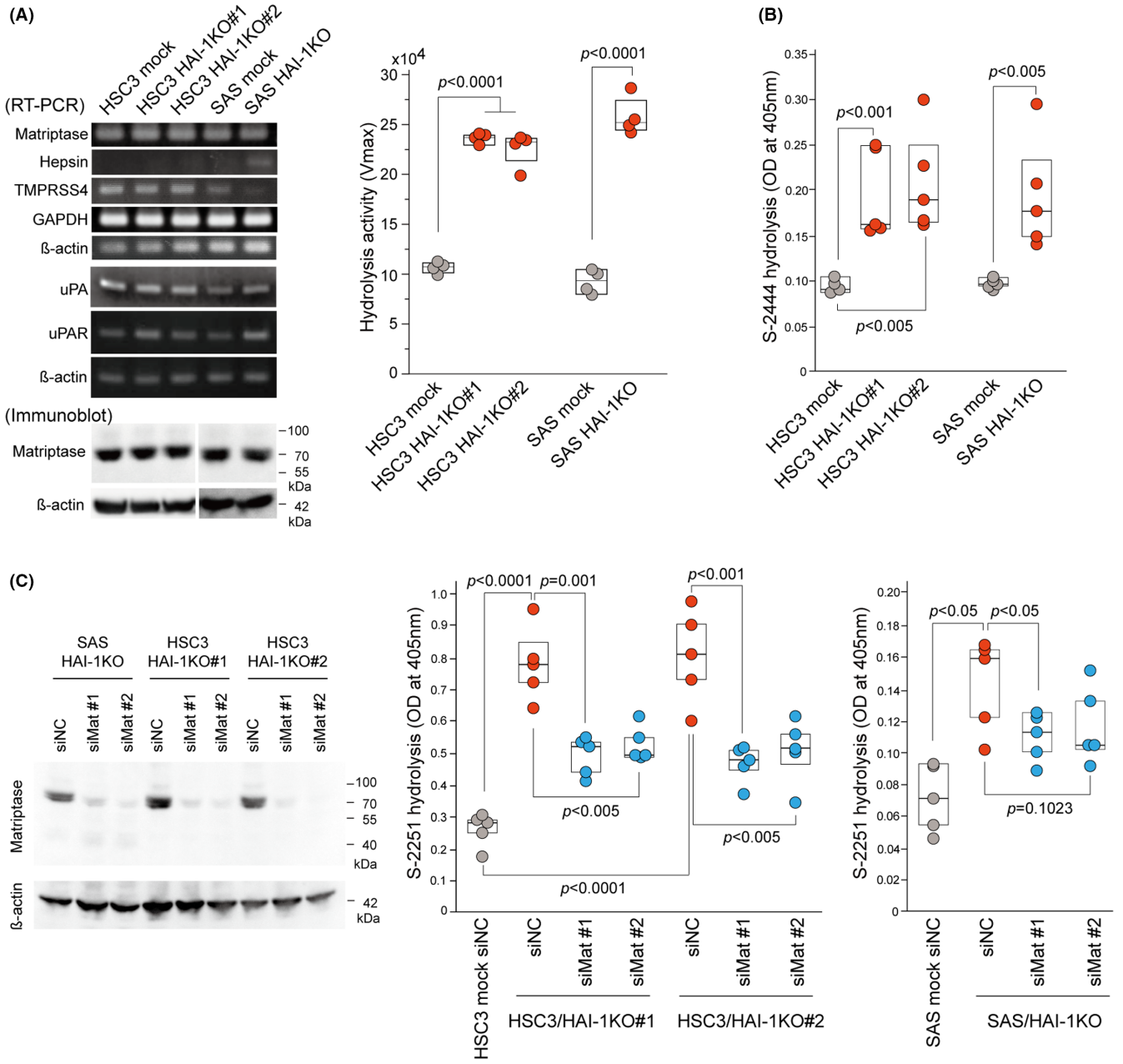

FIGURE 4 Effects of hepatocyte growth factor activator inhibitor type-1 (HAI-1) deficiency on pericellular protease activities. (A) RT-PCR for the expression of matriptase, hepsin and TMPRSS4 mRNAs (left upper panel) and immunoblot for the matriptase protein (left lower panel) in tongue squamous cell carcinoma (TSCC) sublines, and effects of HAI-1 loss on the hydrolysis of synthetic matriptase substrate Boc-Glu-Ala-Arg-AMC by serum-free culture supernatants ($n = 4$; right panel). Vmax, velocity max. (B) Effect of HAI-1 deficiency on pericellular S-2444 hydrolysis ($n = 4$). OD, optical density. (C) Effect of HAI-1 deficiency and matriptase silencing on plasminogen-dependent pericellular S-2251 hydrolysis. Cells were transfected with control siRNA (siNC) or matriptase siRNA (siMat #1 or siMAT #2) and cultured on a 96-well plate. Then the cells were pretreated with 1 μg/mL plasminogen for 3 h, followed by incubation with S-2251 ($n = 5$). The extent of matriptase silencing was verified by immunoblotting of cell lysates (left panel). *p*-values (A–C), Mann–Whitney *U*-test

uPA activity[44] and mRNA levels of uPA and uPA receptor were not altered by the loss of HAI-1, the enhanced uPA activity was likely secondary to the enhanced pericellular activity of pro-uPA-activating protease, particularly matriptase.

Metastasis to the cervical lymph node is an important prognostic factor in head and neck squamous cell carcinomas (HNSCCs), including TSCC.[45] Tumor lymphangiogenesis appears to be correlated with lymph node metastasis of HNSCC.[46] VEGF-C is an important lymphangiogenesis factor in tumors and promotes metastasis,[47] having a significant prognostic impact on HNSCC patients.[46] As such, VEGF-C is secreted as an inactive proform and requires extracellular proteolytic activation to transduce signals through VEGFR-3. Plasmin is the major activator of pro-VEGF-C.[34,35] Our current study indicated that the TSCC cells expressed VEGF-C, and

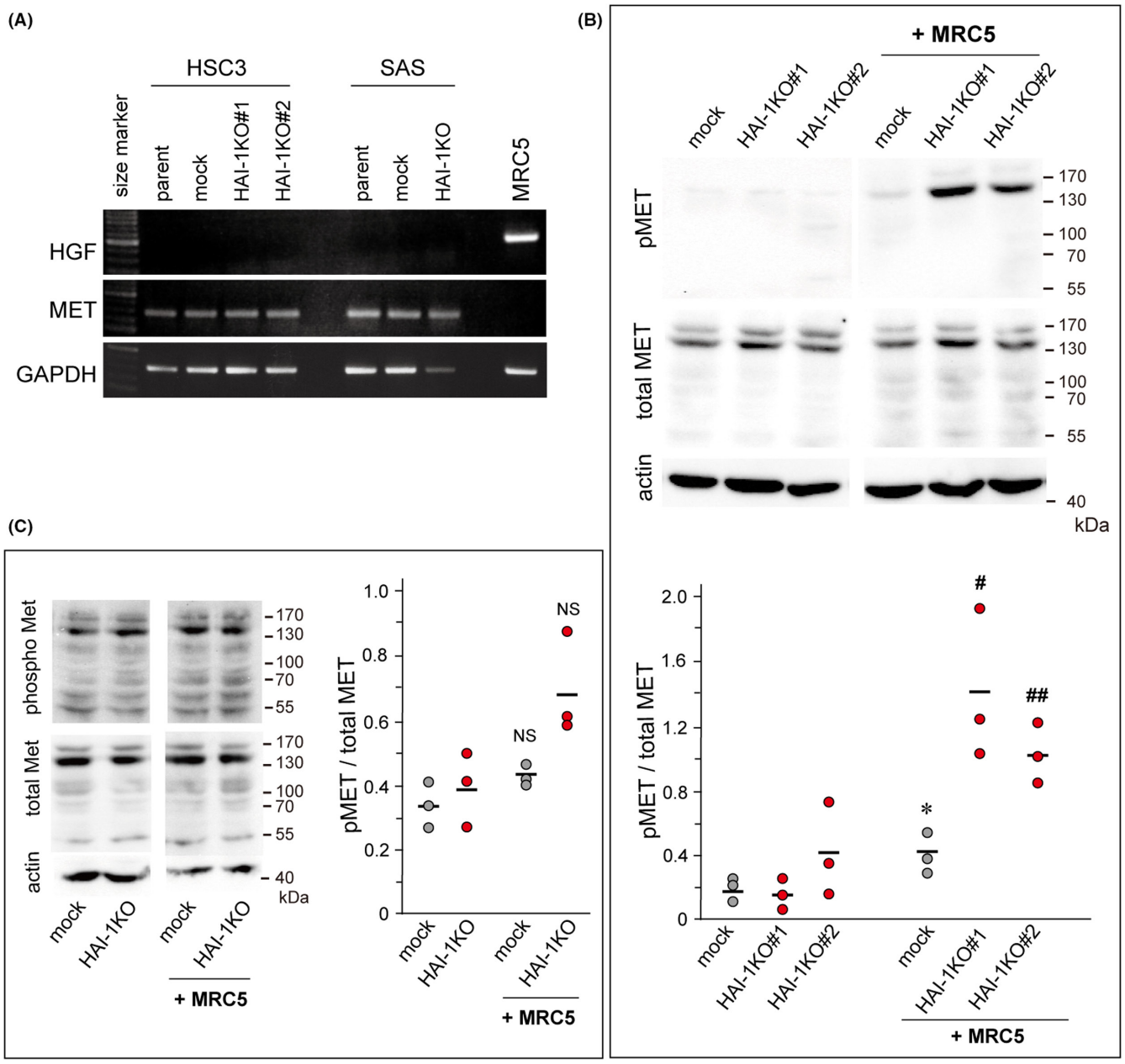

FIGURE 5 Effect of hepatocyte growth factor (HGF) activator inhibitor type-1 (HAI-1) loss on MET phosphorylation in response to co-culture with fibroblasts (MRC5 cells). (A) RT-PCR for the expression of HGF and MET in HSC3 and SAS cell lines (parent) and their sublines. (B) Effect of co-culture of HSC3 sublines and MRC5 on MET phosphorylation. Ratio of phosphorylated MET (pMET) to total MET was calculated and plotted. Data from independent triplicate assays are shown as dots, and horizontal bars represent the mean value. *$P < 0.05$ compared to control (mock) monoculture; #$P < 0.05$ compared to HAI-1KO#1 monoculture and mock + MRC5 co-culture; ##$P < 0.05$ and <0.005 compared to HAI-1KO#2 monoculture and mock + MRC5 co-culture, respectively (Mann-–Whitney *U*-test). (C) Effect of co-culture of SAS sublines and MRC5 cells on MET phosphorylation. NS, not significant compared to corresponding monoculture

the loss of HAI-1 induced enhanced pericellular plasmin generation in the presence of plasminogen and thereby enhanced pro-VEGF-C activation. The increased plasmin generation was likely mediated by enhanced uPA activity, which was induced, at least in part, by dysregulated matriptase activity in the absence of HAI-1. In addition, activity of plasmin, which is inhibited by HAI-1,[44] was further emphasized by the loss of HAI-1. Most of the known physiological target proteases of HAI-1, including matriptase, activate pro-HGF to transduces signals through MET.[4] Collectively, it is reasonable to speculate that HAI-1 insufficiency could lead to concomitant activation of HGF and VEGF-C in the tumor microenvironment in vivo, where stromal pro-HGF and plasma plasminogen are present. The concomitant activation of HGF and VEGF-C may have a synergistic effect on lymphatic invasion and lymph node metastasis of TSCC cells, as suggested by more pronounced lymphangiogenesis resulting from co-activation of MET and VEGFR-3,

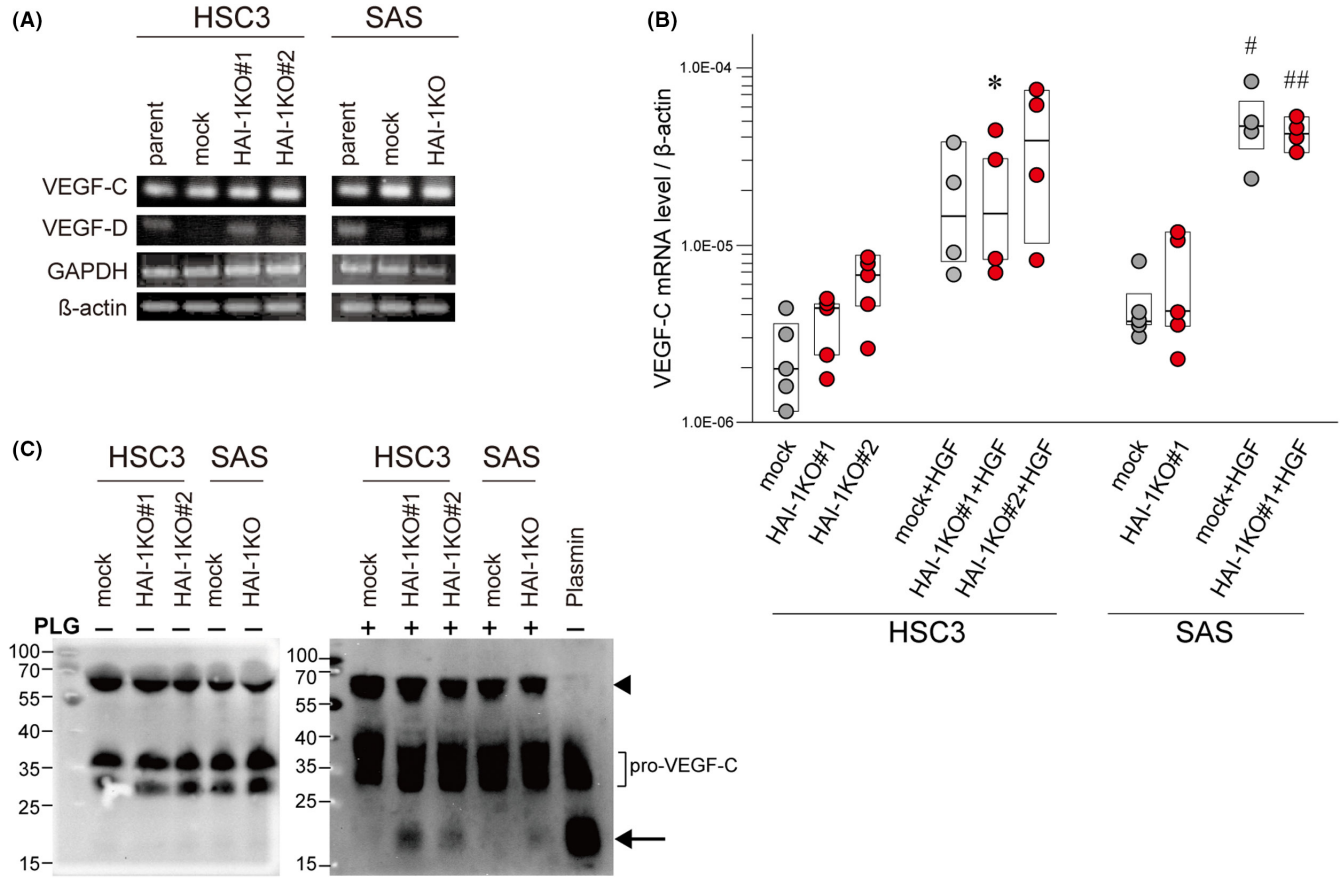

FIGURE 6 Expression of vascular endothelial growth factor-C (VEGF-C) and processing of recombinant pro-VEGF-C. (A) RT-PCR analysis for the expression of VEGF-C and VEGF-D in HSC3 and SAS cells and their sublines. (B) The effect of HGF treatment on the VEGF-C mRNA levels in the cells. *$P < 0.05$; #$P < 0.01$; ##$P < 0.0005$ (Mann–Whitney U-test), compared to corresponding non-treated group. (C) Immunoblot analysis under reducing conditions for the processing of recombinant pro-VEGF-C by culture supernatants of HSC3 and SAS sublines without (–) or with (+) plasminogen (PLG) treatment. Arrow indicates the position of mature VEGF-C. Arrowhead indicates an unprocessed pro-VEGF-C protein band[34]

TABLE 2 Incidence of lymph node (LN) metastasis

Transplanted cell	Total number of mice (Number of sacrificed mice due to >20% weight loss)	Number of mice with LN metastasis (Positive ratio) [Number of metastatic LN in each positive mouse]
SAS		
Control (mock)	10 (0)	5 (50%) [2, 1, 1, 1, 1]
HAI–1KO	10 (0)	9 (90%) [2, 2, 2, 2, 1, 1, 1, 1, 1]
HSC3		
Control (mock)	10 (0)	2 (20%) [1, 1]
HAI–1KO#1	9 (3)	4 (44%) [2, 2, 1, 1]
HAI–1KO#2	9 (3)	4 (44%) [1, 1, 1, 1]
HSC3 + MRC5		
Control (mock) + MRC5	9 (1)	1 (11%) [1]
HAI–1KO#1 + MRC5	10 (5)	3 (30%) [1, 1, 1]
HAI–1KO#2 + MRC5	10 (7)	4 (40%) [3, 1, 1, 1]

compared to the activation of each receptor alone, and the ability of MET signaling to confer cellular responses required for invasive growth of cancer cells.[14,48] Moreover, this study revealed that HGF significantly stimulates the VEGF-C expression in TSCC cells, providing a novel model for an amplifying circuit of growth factors involved in lymphangiogenesis.

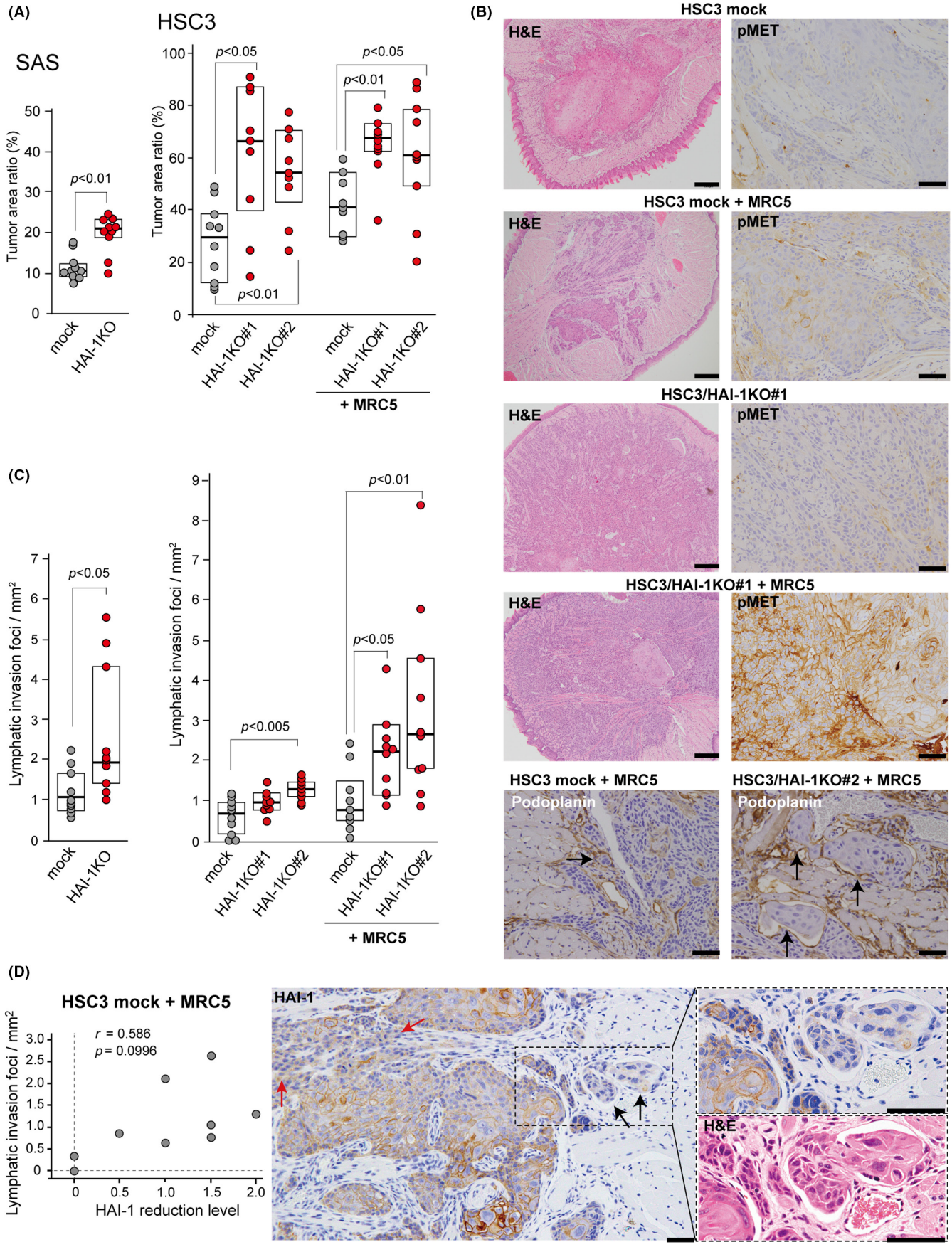
(A)
SAS
Tumor area ratio (%)
p<0.01
mock
HAI-1KO
HSC3
Tumor area ratio (%)
p<0.05
p<0.01
p<0.01
p<0.05
mock
HAI-1KO#1
HAI-1KO#2
+ MRC5
(B)
HSC3 mock
H&E
pMET
HSC3 mock + MRC5
HSC3/HAI-1KO#1
HSC3/HAI-1KO#1 + MRC5
HSC3 mock + MRC5
Podoplanin
HSC3/HAI-1KO#2 + MRC5
Podoplanin
(C)
Lymphatic invasion foci / mm2
p<0.05
p<0.005
p<0.01
p<0.05
(D)
HSC3 mock + MRC5
r = 0.586
p = 0.0996
HAI-1 reduction level
HAI-1
H&E

FIGURE 7 Orthotopic xenotransplantation of SAS and HSC3 HAI-1KO sublines and control (mock) sublines (3×10^5 cells/mouse). HSC3 cells were transplanted with or without 3×10^5 MRC5 cells. (A) Tumor sizes at the time of euthanasia. The size is shown as the ratio (%) of the tumor area to the whole tongue area in an H&E section prepared after autopsy. (B) Representative images of H&E histology, phosphorylated MET (pMET) immunohistochemistry and podoplanin immunohistochemistry of HSC3 tumors in tongue. Arrows indicate lymphatic invasion. Bars, 200 and 50 μm for H&E and immunohistochemistry, respectively. (C) Number of lymphatic invasion foci per 1 mm^2. Circle represents the value of each mouse. (D) Correlation between HAI-1 reduction level and lymphatic invasion in control HSC3 + MRC5 xenografts ($n = 9$, scatter plot). Representative images of decreased membranous HAI-1 in HSC3 cells showing stromal infiltration (red arrows) and lymphatic invasion (black arrows, with higher magnification images at the right side) are also shown. Bars, 50 μm. *p*-values (A,C), Mann–Whitney *U*-test

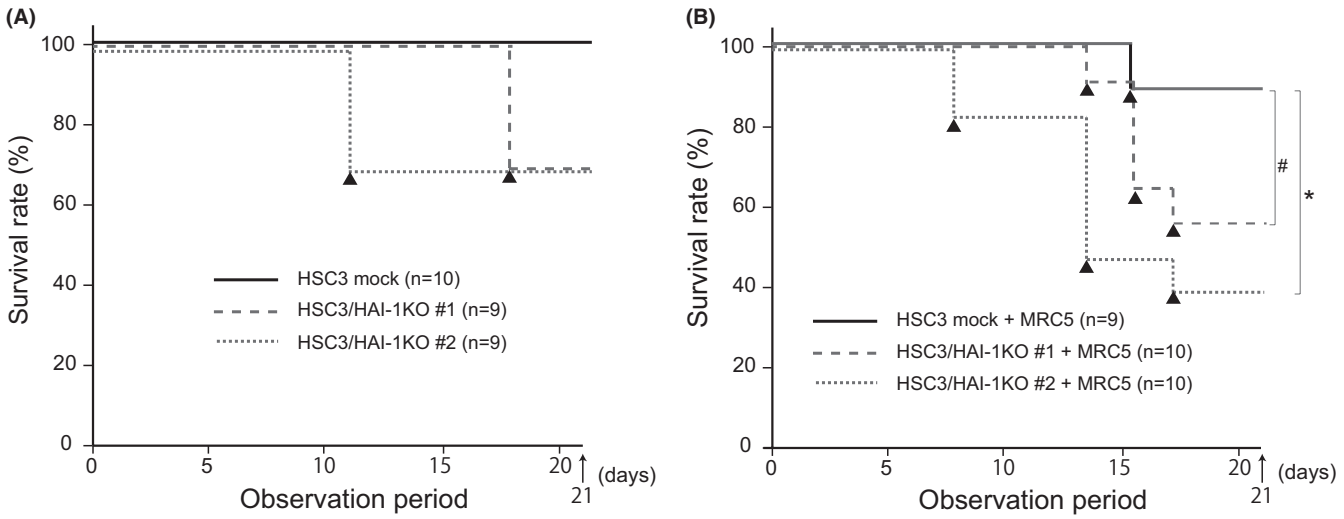

FIGURE 8 Kaplan–Meier survival analysis of mice after xenotransplantation of HSC3 sublines without MRC5 (A) or with MRC5 (B). Arrow heads indicate euthanasia due to weight loss. $^*P < 0.01$; $\#P = 0.075$ (log-rank test)

To further confirm the above in vitro observations, we also performed in vivo orthotopic xenotransplantation experiments in nude mice. The loss of HAI-1 tended to enhance lymphangiogenesis and lymphatic invasion in vivo. For HSC3 cells, which showed stromal pro-HGF-dependent MET phosphorylation in vitro when co-cultured with MRC5 human fibroblasts, co-transplantation with MRC5 significantly enhanced lymphatic invasion of the HAI-1KO sublines.

Our current study has the following limitations. First, our immunohistochemical study of TSCC tissues included a limited number of patients (42 cases), and there was no formal sample size determination. Therefore, we could not perform rigorous statistical analysis regarding the impact of HAI-1 reduction levels on patients' prognosis. Second, the precise molecular mechanisms by which loss of HAI-1 induced invasiveness but decreased the growth rate of TSCC cells in vitro remain to be explored. The enhanced invasion observed in HAI-1KO TSCC cells may be caused by matriptase-dependent pro-uPA activation, as silencing of matriptase reportedly inhibits tumor cell invasion through suppression of uPAR-bound pro-uPA activation.[49] The growth disadvantage following HAI-1 loss in vitro was likely compensated in vivo by tumor microenvironmental factors, as HAI-1KO cells showed a tendency of enhanced tumor growth after orthotopic xenotransplantation. Finally, an in vitro lymphangiogenesis assay to confirm VEGF-C activity was not carried out for this study. Nonetheless, the present study provides, for the first time, evidence that HAI-1 insufficiency may contribute to tumor lymph-angiogenesis and lymphatic invasion.

In summary, the results of this study indicate that the HAI-1 deficiency in TSCC confers excess pericellular proteolysis that could orchestrate robust activation of the HGF/MET pathway and VEGF-C in the tumor microenvironment where stromal pro-HGF and plasma-derived plasminogen are likely present. Activation of cascades of proteases and growth factors following HAI-1 loss shown in this study likely contributes to the lymphatic spreading of cancer cells and may provide potential targets for innovative therapies for TSCC.

ACKNOWLEDGEMENTS

We thank Ms Junko Kurogi for her excellent technical assistance. This work was supported by Japan Society for the Promotion of Science KAKENHI 16H05175 (H.K.) and 20K18483 (K.Y.).

DISCLOSURE

The authors have no conflict of interest.

ORCID

Tsuyoshi Fukushima https://orcid.org/0000-0002-9350-777X
Hiroaki Kataoka https://orcid.org/0000-0001-9948-0451

REFERENCES

1. Sung H, Ferlay J, Siegel RL, et al. Global cancer statistics 2020: GLOBOCAN estimates of incidence and mortality worldwide for 36 cancers in 185 countries. *CA Cancer J Clin*. 2021;71:209-249.
2. Ion Ciucă Mărășescu FI, Marasescu PC, Matei M, et al. Epidemiological and histopathological aspects of tongue squamous cell carcinomas - Retrospective study. *Curr Health Sci J*. 2018;44:211-224.
3. Dolens EDS, Dourado MR, Almangush A, et al. The impact of histopathological features on the prognosis of oral squamous cell carcinoma: a comprehensive review and meta-analysis. *Front Oncol*. 2021;11:784924. doi:10.3389/fonc.2021.784924
4. Kataoka H, Kawaguchi M, Fukushima T, Shimomura T. Hepatocyte growth factor activator inhibitors (HAI-1 and HAI-2): emerging key players in epithelial integrity and cancer. *Pathol Int*. 2018;68:145-158.
5. Shimomura T, Denda K, Kitamura A, et al. Hepatocyte growth factor activator inhibitor, a novel Kunitz-type serine protease inhibitor. *J Biol Chem*. 1997;272:6370-6376.
6. Antalis TM, Buzza MS, Hodge KM, Hooper JD, Netzel-Arnett S. The cutting edge: membrane-anchored serine protease activities in the pericellular microenvironment. *Biochem J*. 2010;428:325-346.
7. Lin CY, Anders J, Johnson M, Dickson RB. Purification and characterization of a complex containing matriptase and a Kunitz-type serine protease inhibitor from human milk. *J Biol Chem*. 1999;274:18237-18242.
8. List K, Szabo R, Molinolo A, et al. Deregulated matriptase causes ras-independent multistage carcinogenesis and promotes ras-mediated malignant transformation. *Genes Dev*. 2005;19:1934-1950.
9. List K, Szabo R, Molinolo A, Nielsen BS, Bugge TH. Delineation of matriptase protein expression by enzymatic gene trapping suggests diverging roles in barrier function, hair formation, and squamous cell carcinogenesis. *Am J Pathol*. 2006;168:1513-1525.
10. Szabo R, Rasmussen AL, Moyer AB, et al. c-Met-induced epithelial carcinogenesis is initiated by the serine protease matriptase. *Oncogene*. 2011;30:2003-2016.
11. Fukushima T, Uchiyama S, Tanaka H, Kataoka H. Hepatocyte growth factor activator: a proteinase linking tissue injury with repair. *Int J Mol Sci*. 2018;19:3435. doi:10.3390/ijms19113435
12. Gherardi E, Birchmeier W, Birchmeier C, Woude GV. Targeting MET in cancer: rationale and progress. *Nat Rev Cancer*. 2012;12:89-103.
13. Boccaccio C, Comoglio PM. MET, a driver of invasive growth and cancer clonal evolution under therapeutic pressure. *Curr Opin Cell Biol*. 2014;31:98-105.
14. Matsumoto K, Umitsu M, De Silva DM, Roy A, Bottaro DP. Hepatocyte growth factor/MET in cancer progression and biomarker discovery. *Cancer Sci*. 2017;108:296-307.
15. Ustach CV, Huang W, Conley-LaComb MK, et al. A novel signaling axis of matriptase/PDGF-D/β-PDGFR in human prostate cancer. *Cancer Res*. 2010;70:9631-9640.
16. Hurst NJ Jr, Najy AJ, Ustach CV, Movilla L, Kim HR. Platelet-derived growth factor-C (PDGF-C) activation by serine proteases: implications for breast cancer progression. *Biochem J*. 2012;441:909-918.
17. Welm AL, Sneddon JB, Taylor C, et al. The macrophage-stimulating protein pathway promotes metastasis in a mouse model for breast cancer and predicts poor prognosis in humans. *Proc Natl Acad Sci USA*. 2007;104:7570-7575.
18. Takeuchi T, Harris JL, Huang W, Yan KW, Coughlin SR, Craik CS. Cellular localization of membrane-type serine protease 1 and identification of protease-activated receptor-2 and single-chain urokinase-type plasminogen activator as substrates. *J Biol Chem*. 2000;275:26333-26342.
19. Le Gall SM, Szabo R, Lee M, et al. Matriptase activation connects tissue factor-dependent coagulation initiation to epithelial proteolysis and signaling. *Blood*. 2016;127:3260-3269.
20. Kilpatrick LM, Harris RL, Owen KA, et al. Initiation of plasminogen activation on the surface of monocytes expressing the type II transmembrane serine protease matriptase. *Blood*. 2006;108:2616-2623.
21. Kanemaru A, Yamamoto K, Kawaguchi M, et al. Deregulated matriptase activity in oral squamous cell carcinoma promotes the infiltration of cancer-associated fibroblasts by paracrine activation of protease-activated receptor 2. *Int J Cancer*. 2017;140:130-141.
22. Hoshiko S, Kawaguchi M, Fukushima T, et al. Hepatocyte growth factor activator inhibitor type 1 is a suppressor of intestinal tumorigenesis. *Cancer Res*. 2013;73:2659-2670.
23. Cheng H, Fukushima T, Takahashi N, Tanaka H, Kataoka H. Hepatocyte growth factor activator inhibitor type 1 regulates epithelial to mesenchymal transition through membrane-bound serine proteinases. *Cancer Res*. 2009;69:1828-1835.
24. Fukushima T, Kawaguchi M, Yamasaki M, Tanaka H, Yorita K, Kataoka H. Hepatocyte growth factor activator inhibitor type 1 suppresses metastatic pulmonary colonization of pancreatic carcinoma cells. *Cancer Sci*. 2011;102:407-413.
25. Borowicz S, Principe DR, Dorman MJ, et al. HAI-1 is an independent predictor of lung cancer mortality and is required for M1 macrophage polarization. *PLoS One*. 2021;16:e0252197. doi:10.1371/journal.pone.0252197
26. Baba T, Kawaguchi M, Fukushima T, et al. Loss of membrane-bound serine protease inhibitor HAI-1 induces oral squamous cell carcinoma cells' invasiveness. *J Pathol*. 2012;228:181-192.
27. Fukushima T, Kawaguchi M, Yamamoto K, et al. Aberrant methylation and silencing of the *SPINT2* gene in high-grade gliomas. *Cancer Sci*. 2018;109:2970-2979.
28. Kataoka H, Suganuma T, Shimomura T, et al. Distribution of hepatocyte growth factor activator inhibitor type 1 (HAI-1) in human tissues. Cellular surface localization of HAI-1 in simple columnar epithelium and its modulated expression in injured and regenerative tissues. *Histochem Cytochem*. 1999;47:673-682.
29. Yamamoto K, Kawaguchi M, Shimomura T, et al. Hepatocyte growth factor activator inhibitor type-2 (HAI-2)/*SPINT2* contributes to invasive growth of oral squamous cell carcinoma cells. *Oncotarget*. 2018;9:11691-11706.
30. Kawaguchi M, Kanemaru A, Sawaguchi A, et al. Hepatocyte growth factor activator inhibitor type 1 maintains the assembly of keratin into desmosomes in keratinocytes by regulating protease-activated receptor 2-dependent p38 signaling. *Am J Pathol*. 2015;185:1610-1623.
31. Dass K, Ahmad A, Azmi AS, Sarkar SH, Sarkar FH. Evolving role of uPA/uPAR system in human cancers. *Cancer Treat Rev*. 2008;34:122-136.
32. Zhao D, Wang S-H, Feng Y, Hua C-G, Zhao J, Tang X-F. Intratumoral c-Met expression is associated with vascular endothelial growth factor C expression, lymphangiogenesis, and lymph node metastasis in oral squamous cell carcinoma: implications for use as a prognostic marker. *Hum Pathol*. 2011;42:1514-1523.
33. Joffre C, Barrow R, Ménard L, Calleja V, Hart IR, Kermorgant S. A direct role for Met endocytosis in tumorigenesis. *Nat Cell Biol*. 2011;13:827-837.
34. Rauniyar K, Jha SK, Jeltsch M. Biology of vascular endothelial growth factor C in the morphogenesis of lymphatic vessels. *Front. Bioeng. Biotechnol*. 2018;6:7. doi:10.3389/fbioe.2018.00007
35. Künnapuu J, Bokharaie H, Jeltsch M. Proteolytic cleavages in the VEGF family: generating diversity among angiogenic VEGFs, essential for the activation of lymphangiogenic VEGFs. *Biology (Basel)*. 2021;10:167. doi:10.3390/biology10020167
36. Zhang YW, Su Y, Lanning N, et al. Enhanced growth of human met-expressing xenografts in a new strain of immunocompromised mice transgenic for human hepatocyte growth factor/scatter factor. *Oncogene*. 2005;24:101-106.
37. Tanaka H, Nagaike K, Takeda N, et al. Hepatocyte growth factor activator inhibitor type 1 (HAI-1) is required for

branching morphogenesis in the chorioallantoic placenta. *Mol Cell Biol*. 2005;25:5687-5698.
38. Nagaike K, Kawaguchi M, Takeda N, et al. Defect of hepatocyte growth factor activator inhibitor type 1/serine protease inhibitor, Kunitz type 1 (Hai-1/Spint1) leads to ichthyosis-like condition and abnormal hair development in mice. *Am J Pathol*. 2008;173:1464-1475.
39. Szabo R, Molinolo A, List K, Bugge TH. Matriptase inhibition by hepatocyte growth factor activator inhibitor-1 is essential for placental development. *Oncogene*. 2007;26:1546-1556.
40. Szabo R, Kosa P, List K, Bugge TH. Loss of matriptase suppression underlies spint1 mutation-associated ichthyosis and postnatal lethality. *Am J Pathol*. 2009;174:2015-2022.
41. Domoto T, Takino T, Guo L, Sato H. Cleavage of hepatocyte growth factor activator inhibitor-1 by membrane-type MMP-1 activates matriptase. *Cancer Sci*. 2012;103:448-454.
42. Ishikawa T, Kimura Y, Hirano H, Higashi S. Matrix metalloproteinase-7 induces homotypic tumor cell aggregation via proteolytic cleavage of the membrane-bound Kunitz-type inhibitor HAI-1. *J Biol Chem*. 2017;292:20769-20784.
43. Shiomi T, Okada Y. MT1-MMP and MMP-7 in invasion and metastasis of human cancers. *Cancer Metast Rev*. 2003;22:145-152.
44. Kataoka H, Miyata S, Uchinokura S, Itoh H. Roles of hepatocyte growth factor (HGF) activator and HGF activator inhibitor in the pericellular activation of HGF/scatter factor. *Cancer Metastasis Rev*. 2003;22:223-236.
45. Thomson PJ. Perspectives on oral squamous cell carcinoma prevention-proliferation, position, progression and prediction. *J Oral Pathol Med*. 2018;47:803-807. doi:10.1111/jop.12733
46. Karatzanis AD, Koudounarakis E, Papadakis I, Velegrakis G. Molecular pathways of lymphangiogenesis and lymph node metastasis in head and neck cancer. *Eur Arch Otorhinolaryngol*. 2012;269:731-737.
47. Mandriota SJ, Jussila L, Jeltsch M, et al. Vascular endothelial growth factor-C-mediated lymphangiogenesis promotes tumour metastasis. *EMBO J*. 2001;20:672-682.
48. Gibot L, Galbraith T, Kloos B, et al. Cell-based approach for 3D reconstruction of lymphatic capillaries in vitro reveals distinct functions of HGF and VEGF-C in lymphangiogenesis. *Biomaterials*. 2016;78:129-139. doi:10.1016/j.biomaterials.2015.11.027
49. Suzuki M, Kobayashi H, Kanayama N, et al. Inhibition of tumor invasion by genomic down-regulation of matriptase through suppression of activation of receptor-bound pro-urokinase. *J Biol Chem*. 2004;279:14899-14908.

SUPPORTING INFORMATION

Additional supporting information may be found in the online version of the article at the publisher's website.

How to cite this article: Izumi A, Yamamoto K, Kawaguchi M, et al. Insufficiency of hepatocyte growth factor activator inhibitor-1 confers lymphatic invasion of tongue carcinoma cells. *Cancer Sci*. 2022;113:2179–2193. doi:10.1111/cas.15346